

# Periodic Nulls in Pulsar B1133+16

Jeffrey L. Herfindal and Joanna M. Rankin

*Physics Department, University of Vermont, Burlington, VT 05405\**

Accepted 2007 month day. Received 2007 month day; in original form 2007 month day

## ABSTRACT

Numerous studies of the brightest Cambridge pulsar, B1133+16, have revealed little order in its individual pulses, apart from a weak 30-odd-rotation-period fluctuation feature and that some 15% of the star’s pulses are “nulls.” New Arecibo observations confirm this feature and that it modulates all the emission, not simply the “saddle” region. By quenching all subpulse modulation, we demonstrate that the star’s “null” pulses exhibit a similar periodicity. A carousel model with a sparse and irregular “beamlet” population appears to be compatible with these characteristics.

**Key words:** miscellaneous – methods: — data analysis – pulsars: general, individual (B1133+16)

## 1 INTRODUCTION

PSR B1133+16 has been the subject multiple studies, in part, because it is the brightest of the first four Cambridge pulsars . It exhibits a classic double profile along with the usual S-shaped polarization-angle (hereafter PA) transverse.

Early individual pulse studies of B1133+16 noted a long period modulation feature (Slee & Mulhall 1970; Taylor & Huguenin 1971, hereafter SM70 & TH71), but its significance was uncertain because the pulsar shows little orderly subpulse structure. Refractive scintillation also corrugates the pulsar’s intensity strongly at meter wavelengths. Making some effort to mitigate its effects, Backer (1973, hereafter B73) found this feature strongest in the “saddle” region and measured its period to be 37 stellar rotation periods (hereafter  $P_1$ ). Both TH71 and Backer found, in the latter’s words, “a weak ordering process which correlates the emission in a series of pulses.” This consisted of “single subpulses in component I or component II, subpulses in both components, and pulses with no emission.” The subpulses with no emission—dubbed “nulls” by Backer (1970)—were found to occur around 15% of the time .

Little regular or consistent subpulse *drift* has been identified in B1133+16, although its sightline traverse is sufficiently oblique that this would not be ruled out . B73 followed SM70 in reporting a weak and occasional 0.20 cycle/period (hereafter  $c/P_1$ ) feature; and, Taylor *et al.* (1975), using correlation methods, found a weak preference for positive subpulse motion in adjacent pulses.

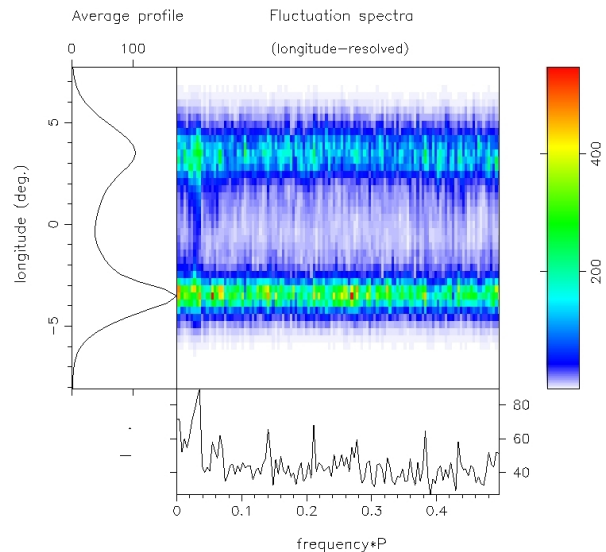


**Figure 1.** Typical longitude-resolved fluctuation spectra (hereafter LRF) for PSR B1133+16, computed in total power (Stokes  $I$ ) for the 327-MHz observation (“D” in Table 1) on 2006 October 10. The main panel gives the spectra according to the average profile in the left panel, and the integrated spectrum is shown in the bottom panel. Here, an FFT length of 256 was used.

More recently, Nowakowski (1996) identified very occasional intervals during which subpulses appeared to drift progressively across the profile in about 12  $P_1$ , usually positively.

\* J.Herfindal@gmail.com; Joanna.Rankin@uvm.edu

**Table 1.** Observational parameters.

Observation	Date m/d/yr	Resolution (degrees/sample)	Length (pulses)
A	07/20/03	0.16	1517
B	11/28/05	0.18	2021
C	11/29/05	0.18	2695 <sup>a</sup>
D	10/07/06	0.35	1934

<sup>a</sup> The first 500 pulses of this observation were ignored due to noticeable interference.

Both Nowakowski and Weltevrede (2007)<sup>1</sup> identify the low frequency feature, and show that its effect is not confined to the “saddle” region, but modulates all of the star’s emission. They further determine its period to be  $33 \pm 3 P_1$ , as we also illustrate in Figure 1.

Several other recent papers piqued a renewed interest in pulsar B1133+16: First, Bhat *et al.* (2007) demonstrated that the star’s null pulses are not strictly simultaneous at all frequencies. They found an about 5% excess of nulls which only occurred at frequencies below or near 1.4 GHz. Second, the pulsar was found to produce broadband “giant” pulses (Kramer *et al.* 2003) on the trailing edge of the leading component about 1% of the time (at 4850 MHz). And third, on no other basis than the above studies, Gil *et al.* (2006) claimed that the  $33 P_1$  modulation represents a carousel circulation time, and we strongly doubted that this was the case.

In order to further explore the significance of this low frequency modulation, we have analyzed a series of recent, high quality observations from the Arecibo Observatory in Puerto Rico. In §2 we describe these observations, and §3 presents the analysis. A discussion and summary of the results is then given in §4.

## 2 OBSERVATIONS

The observations were carried out using the 305-meter Arecibo Telescope in Puerto Rico. All of the observations used the upgraded instrument with its Gregorian feed system, 327-MHz (P band) receiver, and Wideband Arecibo Pulsar Processor (WAPP<sup>2</sup>). The ACFs and CCFs of the channel voltages produced by receivers connected to orthogonal linearly (circularly, after 2004 October 11) polarized feeds were 3-level sampled. Upon Fourier transforming, some 64 channels were synthesized across a 25-MHz bandpass with about a milliperiod sampling time. Each of the Stokes parameters was corrected for interstellar Faraday rotation, various instrumental polarization effects, and dispersion. The date, resolution, and the length of the observations are listed in Table 1.

<sup>1</sup> Or, see Weltevrede *et al.* (2006,2007).

<sup>2</sup> <http://www.naic.edu/~wapp>

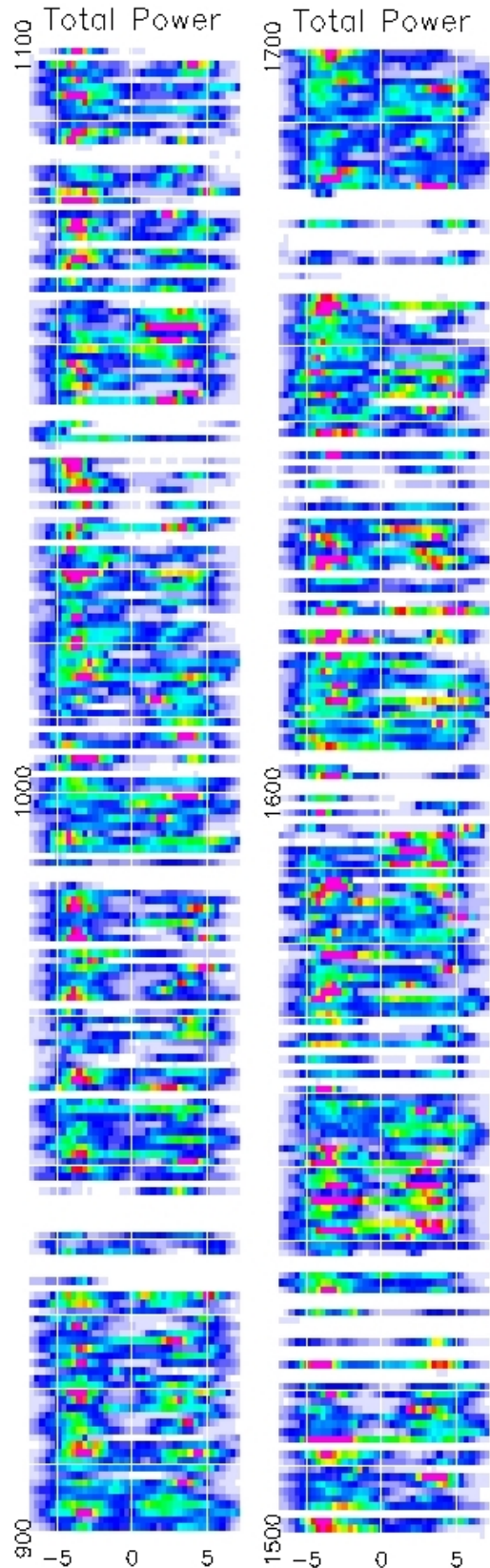


**Figure 2.** Total power (Stokes *I*) displays extracted from observation “D” in Table 1, pulses 901-1100 (left) and 1501-1700 (right), color coded as in Fig. 1, but saturating in magenta.

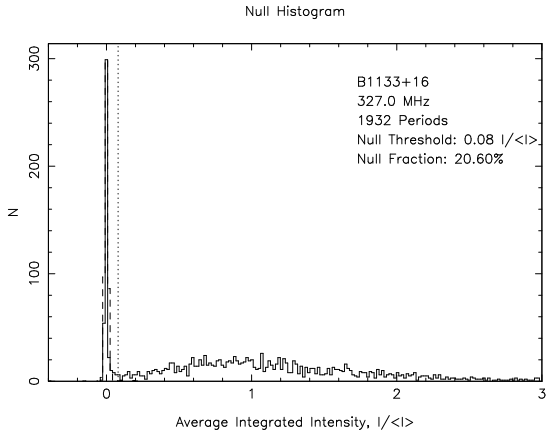


**Figure 3.** Null frequency histogram for the “D” observation in Table 1. The integrated-intensity distribution of the pulses (solid line) and that of the off-pulse region (dashed line) are plotted. The plot is truncated at high intensity in order to show the detail near zero (it extends to  $>10 I/\langle I \rangle$ ). The vertical dotted line represents a plausible threshold of  $0.08 I/\langle I \rangle$  for distinguishing the nulls. Note that even with this very large signal-to-noise ratio, the null distribution is continuous with that of the pulses. In part, the pulse and null distributions are conflated by interstellar scintillation (hereafter ISS) effects, but the D observation is the least corrugated in this respect. Two pulses were ignored due to bad baselines.

### 3 ANALYSIS

#### 3.1 Nulls, Partial Nulls, and Giant Pulses

B1133+16 is known to produce a classic double profile with a taller leading and a wider trailing component (at 327 MHz) as seen in the left panel of Fig. 1. Despite its prominence and brightness, little regular or consistent order in the star’s subpulses has been identified, perhaps because of their exceptionally sporadic character.<sup>3</sup> Two 200-pulse sequences (hereafter PSs) of our least ISS-corrugated observation (“D” in Table 1) are shown in Fig. 2. The nulls are more than obvious—given the typical  $>100:1$  signal-to-noise ratio (hereafter S/N)—as white intervals between the pulses. Figure 3 gives a pulse-intensity histogram for this observation. Notice the strong presence of pulses with zero (or near zero) aggregate intensity. However, note well also that the distribution is continuous between the pulses and nulls, frustrating any possibility of delineating the two populations positively. The dotted line then represents a conservative boundary at  $0.08 \langle I \rangle$ . Accordingly, 20.6% of the pulses fall below this threshold, and a considerable portion of these, we know, are “partial nulls”—that is, affecting only the leading or trailing component. The frequency of such partial nulls is readily estimated either by eye using dis-

<sup>3</sup> The giant-pulse peaks in Fig. 2 are difficult to see because they are so brief and distinguished by magenta rather than red coding. Nonetheless, they dominate the leading component in pulses 542, 1546, and 1574 and trailing in pulse 1000 and 1682.

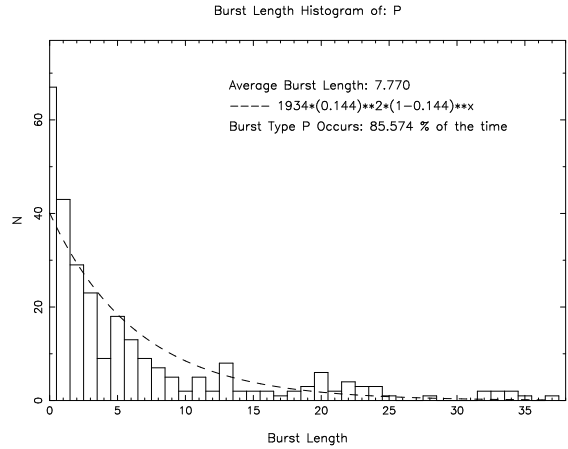


**Figure 4.** Histogram of burst lengths for observation D (solid curve). A “burst” is defined as the number of contiguous pulses between full nulls, and successive full nulls are counted as bursts of zero length. The expected burst frequency is then computed statistically and plotted according to the dashed curve. Note the overabundance of very short (including zero) and very long bursts.

plays such as those in Fig. 2 or by computing intensity distributions separately for the profile halves. Some of these partial nulls are clearly visible in the latter figure, notably pulses 935, 988, 1561, 1675, and 1681. Partial null occurrence is about 7% in each of the “D” components, wildly more frequent than would be expected randomly. A corresponding estimate for the full nulls is 14.4%. All of the observations are consistent with the null fraction found by Ritchings (1976) and have a partial null fraction of 5 to 8%.

A histogram of burst length is shown in Figure 4, where a “burst” is defined as the number of contiguous pulses between full nulls—and successive full nulls are counted as having burst-length zero. A theoretical curve is also plotted (dashed line), giving the expected occurrence assuming 14.4% randomly distributed nulls. Notice the pronounced overabundance of very short (including zero) bursts as well as very long ones. A further look at Fig. 2 reveals that many of the nulls occur in short groups separated by equally short bursts, with an overabundance of contiguous nulls. Histograms of null length (not shown) verify that a null length of one is, by far, most frequent and that the nulls never persist longer than 3 or 4 periods.

#### 3.2 The Low Frequency Feature

The longitude-resolved fluctuation (hereafter LRF) spectra given above in Fig. 1 is typical of our several observations. The low frequency feature is often broad and non-descript and sits atop a nearly “white” continuum. We also see clearly here that the feature modulates both the components and the “saddle” region. LRF spectra reflect not only the pulsar’s “normal” emission properties but also its giant pulses and the often severe corrugation produced by ISS. Given these several, even dominating

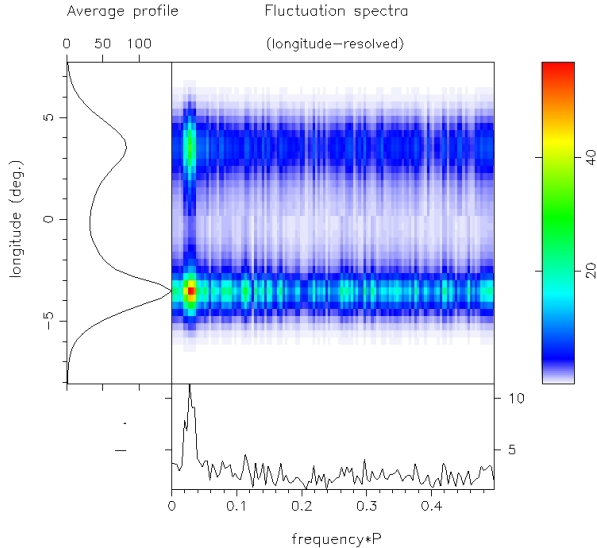


**Figure 5.** LRF spectra of the artificial “PMQ” PS corresponding to observation “D”. Here, most pulse modulation was quelled by substituting a scaled-down average profile for the pulses and a similarly scaled half-average profile for the emission during partial nulls (see text).

distortions, one can well be surprised that any consistent modulation feature survives at all. However, every fluctuation study in the literature notes this low frequency modulation, and the recent work of both Nowakowski (1996) and Weltevrede (2007) measure a fairly consistent period of  $33 \pm 3 P_1$ .

LRF (Stokes  $I$ ) power spectra were computed for all the observations in Table 1 using Fourier transforms of length 256. One or several 30-odd  $P_1$  features was prominent in all of them and fell close to the values given in Table 2. The individual PSs (and sections of them) show other minor features, but only the  $0.20 c/P_1$  noted by Backer was at all consistent (appearing in all but “B”).

### 3.3 Pulse-Modulation Quelling (PMQ)

What would B1133+16’s LRF spectra be able to tell us were there no giant pulses nor ISS to contend with? We find it curious that these effects do not (much) degrade our ability to distinguish the star’s nulls from pulses (given the exceptionally high S/N), but they tend to obscure what useful information the LRF spectra may have held. With these questions in mind we investigated whether some compression of the PS’s amplitude distribution might be useful. Then we asked whether eliminating all the pulse modulation could be revealing? The latter might entail computing the power spectrum of the binary series of nulls and non-nulls. Given the centrality of the two component’s individual behaviour, however, we decided to try suppressing all pulse modulation except that implied by the star’s partial nulls.

We then constructed artificial PS corresponding to each of the natural ones as follows: Each had been scrutinized, pulse by pulse, in order to make reliable estimates of the sequences of pulses, full, and partial nulls. Color displays such as that in Fig. 2 provided a convenient and

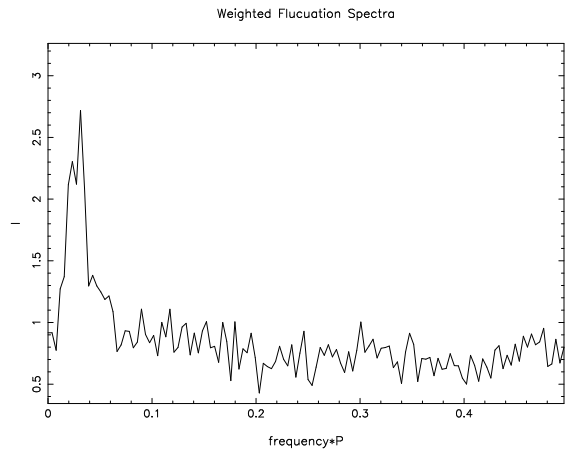


**Figure 6.** Weighted fluctuation power spectrum of the combined PMQ LRF spectra. The aggregate LRF spectra of the observations in Table 2 were weighted by the square of their lengths, which we took as approximately proportion to their respective total pulsar energy.

quantitative measure of pulse intensity because the noise levels of the observations fall just inside the white region at the low intensity end of the color bar. (Artificial PSs generated using an appropriate threshold give very similar results, but given the continuity of intensity at very low intensity, it was useful to assess all the pulses with energies in the threshold region.)

Then, the actual generation of the artificial PSs was trivial: a) a suitably scaled down average profile was substituted in place of every pulse, and b) a similarly scaled half-average pulse was substituted for the partial null emission. The only slight complexity was that the leading and trailing half-average profiles were tapered over  $2\text{--}3^\circ$  in the “saddle” region (while keeping their sum that of the full profile) to avoid inserting a step function.

### 3.4 Periodic Nulls?!

LRF spectra were computed for each of the four artificial PMQ PSs corresponding to the natural PSs in the two tables, and an example is given as Figure 5. As might be expected, the level of “white” fluctuation power is greatly reduced—*cf.* Fig. 1. Our surprise was that the low frequency feature persisted, and in some cases was even stronger. Thus its S/N is considerably greater. The periods of the features obtaining from the four LRF analyses, together with their estimated errors, are collected into Table 2. The range among the four values suggests some actual variation, but this is far from certain, in particular because most of the low frequency responses appeared to have some structure with 2-3 strong peaks. (Identical LRF results were obtained, as expected after some thought, when the nulls were filled as above with profiles and the regions of emission with noise.)

Taking a further step to explore the significance of these various responses, we computed a weighted-average of the PMQ LRFs, which is given as Figure 6. Here, the primary peak is at  $32 P_1$ , the secondary one at some  $43$

**Table 2.** Observed low frequency feature after PMQ.

Observation	Main Feature
A	$28 \pm 2 P_1$
B	$32 \pm 2 P_1$
C	$39 \pm 3 P_1$
D	$36 \pm 3 P_1$
Weighted LRF	$32 \pm 2 P_1$

$P_1$ , and one can also see a “band” of fluctuation power extending down to  $25 P_1$ . In an effort to weight the four observations appropriately, we used the square of their lengths, this assuming that length was approximately proportional to total pulsar energy.

The conclusion to be drawn here, apparently, is that the nulls themselves reflect whatever underlying periodicity is responsible for the low frequency feature. Or, conversely, the aggregate fluctuation power of the low frequency feature is little changed whether the pulse modulation is quelled or not, implying that the feature fluctuations are *produced* by the nulls! These conclusions are perplexing because (with very unusual exceptions) no obvious or regular periodicities have heretofore been attributed to null occurrence.

### 3.5 Could a Rotating Subbeam Carousel Produce the Periodic Nulls?

It may seem strange that an irregularly filled rotating-subbeam carousel with a continually changing “beamlet” configuration could give rise to a well defined feature corresponding to its circulation time ( $\hat{P}_3$ ). However, little more is required than a) that the beamlet pattern be sparsely populated (and thus highly modulated) and that b) it remain relatively stable over a few rotations. If then, the main fluctuation feature in Figure 6 provides an estimate of this circulation time, its width gives us an indication of the modulation’s phase and amplitude stability.

Figure 7 shows two typical intervals folded at the putative  $\hat{P}_3$  period. Here, the local value is  $28.44 P_1$  and the PS is folded over four rotations or  $113 P_1$ . As expected, the two patterns are very different. However, most similar folds exhibit two common properties: first, they show “null zones” where the aggregate power is negligible—implying “negative” fluctuation power at this period—and, second, they are highly modulated with “positive” fluctuation power at the fundamental period.

Whatever the detailed configuration of the carousel, its lowest angular-frequency component—corresponding to a full rotation in magnetic azimuth through our sightline—will contribute to the LRF feature as long as a) the power is fully modulated by a “sparse” beamlet population, and b) these beamlets are roughly stable for several rotations. A “forest” of other responses, of course, would be produced by the finer structure of the carousel configuration. However, these will be attenuated and “whitened” over a few rotations as the con-

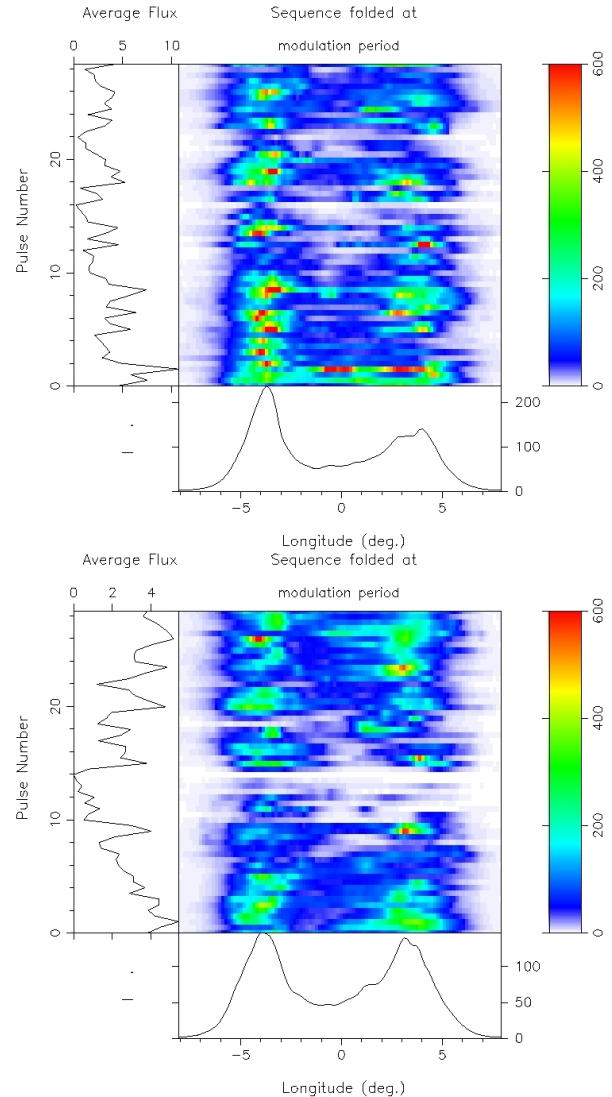


**Figure 7.** Typical 113-pulse intervals of observation (A in Table 1) folded at the local  $28.44 P_1$  putative value of  $\hat{P}_3$ . Each display represents the average of four such intervals. Note that both folded PSs show one or more “null zones” where the intensity is negligible as well as maxima that are 3-5 times larger than the average.

figuration continually changes. We note again the large bias of roughly “white” fluctuation power on which the low frequency features sit in each of the spectra above.

It may still seem paradoxical that the nulls alone produce an LRF feature of the same frequency when all the pulse modulation is suppressed by the profile-filling (PMQ) method above. However, we can now see that the “nulls” arise in just the same manner as the pulse modulation—that is, from the sparsely filled carousel-beam pattern. Moreover, B1133+16’s nulls appear to exhibit just the properties one would expect from this origin: a) the energy distribution is continuous between pulses and nulls, b) both full and partial nulls occur with comparable frequency, and c) null (or burst) occurrence is hardly random.

#### 4 SUMMARY AND DISCUSSION

In the foregoing sections we have shown that pulsar B1133+16's roughly  $32-P_1$  modulation is a key property of its emission. Though weak fluctuation at this period had been identified long ago, several factors seem to have prevented full realization of its importance. This modulation tends to be “washed out” both by the strong diffractive scintillation of this low dispersion-measure star and within its two bright components by strong (and “giant”-pulse) fluctuations, to the end that it was falsely associated only with the central saddle region (*e.g.*, Rankin 1986). This paper confirms the recent realization that both components and the saddle region are modulated at this rate. It also shows that both the pulse emission and nulls share this modulation period.

While we cannot fully prove that the star's roughly  $32-P_1$  modulation reflects the properties of a subbeam carousel rotating through our sightline, we are able to show that the characteristics of the modulation are fully compatible with this interpretation. Given the pulsar's usual lack of perceptible drift or other  $P_3$  signature, the putative carousel must usually be comprised of irregular and sparsely spaced beamlets—and we also see that such configuration must be stable over intervals longer than 30 and probably not much more than  $100 P_1$ .

Our analysis can say little more about the star's pulsed emission, but there is a good deal more to say about the star's nulls. First, they usually last only a single period and never more than three or four. Second, their pulse-energy distribution is continuous with that of the null distribution—or said differently, a small population of very weak pulses bridges the intensity distribution between the roughly 15% nulls and the weak edge of the pulse-energy distribution. Third, the nulls are not randomly distributed within the pulsar's PSs, and we see this in two different ways: a) while the long nulls are only a few pulses, there are far too many contiguous nulls, and b) the nulls themselves show exactly the same  $32-P_1$  periodicity as the pulses. Four, there are far too many partial nulls, as the region around each component exhibits some 20% nulls.

The striking thing about B1133+16's null periodicity is that the pulsar's PSs are otherwise almost completely irregular; no drift of other consistent modulation has ever been identified. “How then can the nulls be periodic?” we asked ourselves! The answer, we now believe, can be found in a sparsely populated subbeam carousel whose beamlet configuration remains relatively constant over several circulation times.

This said, there are a growing number of other pulsars with nulling effects which may well be related: Redman *et al.* (2005) noted that B2303+30's nulls mostly occur in the star's weaker ‘Q’ mode, and that this mode alternates with the bright ‘B’ mode in a quasi-periodic manner. B0834+06's nulls are also cyclic in that they occur in synchrony with the star's  $2.17-P_1$  primary PS modulation (Rankin & Wright 2007a); whereas in J1819+1305 long nulls alternate with intervals of bright emission such that overall the nulls appear to be highly periodic (Rankin & Wright 2007b). The weeks-long, quasi-periodic nulls of B1931+24 have been de-

tected in the pulsar's timing as spindown-torque decreases (Kramer *et al.* 2006). And, finally, Wang *et al.* (2007) have studied a group of pulsars known for their long nulls from timing efforts, and some of these also exhibit clear periodicities.

Finally, we expect that the carousel model for B1133+16's nulls is fully compatible with their frequency dependence as so ably demonstrated by Bhat *et al.* above. The salient issue, probably, is that the excess nulls occur at lower frequencies where the carousel's angular dimensions are greater. Their larger configurations may have more interstitial space (or “null zones”) where “empty” sightline traverses through the beamlet pattern can occasionally occur. This scenario further seems compatible with Bhat *et al.*'s finding that the star's low frequency nulls show only weak emission at high frequency, because if the sightline misses beamlets at low frequency, it may only graze them at higher ones.

It could then not be clearer, in summary, that pulsarists still have much to learn about pulsar nulling. And, as regards the Gil *et al.*'s circulation-time interpretation for B1133+16, we have eaten our hats!

#### ACKNOWLEDGMENTS

We thank Dipanjan Mitra and Geoffrey Wright for their critical readings of the paper in manuscript and Stephen Redman for assistance with the analyses. Portions of this work were carried out with support from US National Science Foundation Grant AST 99-87654. Arecibo Observatory is operated by Cornell University under contract to the US NSF. This work used the NASA ADS system.

#### REFERENCES

- Backer, D. C. 1973, *Ap.J.*, 182, 245  
 Bhat, N.D.R., Gupta, Y., Kramer, M., Karastergiou, A., Lyne, A.G., & Johnston, S. 2007, *A&A*, 462, 257  
 Deshpande, A.A., Rankin, J.M., 2001, *MNRAS*, 322, 438  
 Gil, J., Melikidze, G., Zhang, B., 2006 *A&A*, 457, L5  
 Kramer, M., Karastergiou, A., Gupta, Y., Johnston, S., Bhat, N.D.R., & Lyne, A.G. 2003, *A&A* 407, 655  
 Kramer, M., Lyne, A. G., O'Brien, J. T., Jordan, C. A., & Lorimer, D. R. 2006, *Science*, 312, 549  
 Nowakowski, L., 1996, *Ap.J.* 457, 868  
 Pilkington, J.D.H., Hewish, A., Bell, S. J. & Cole, T. W., 1968, *Nature*, 218, 126  
 Rankin, J.M., 1986, *Ap.J.*, 301, 901  
 Rankin, J.M., 1993a, *Ap.J.*, 405, 285  
 Rankin, J.M., 1993b, *Ap.J. Suppl.*, 85, 145  
 Rankin, J. M. & Wright, G.A.E. 2007a, *MNRAS*, in press  
 Rankin, J. M. & Wright, G.A.E. 2007b, *MNRAS*, preprint  
 Redman, S.R., Wright, G.A.E., Rankin, J.M., 2005, *MNRAS*, 375, 859  
 Ritchings, R.T. 1976, *MNRAS*, 176, 249  
 Slee, O.B., Mulhall, P.S., 1970, *Proc. Astr. Soc. Australia*, 1, 322

- Taylor, J. H., Huguenin, G. R. 1971, *Ap.J.*, 167, 273  
 Taylor, J. H., Manchester, R. N., Huguenin, G. R. 1975, *Ap.J.*, 195, 513  
 Wang, N., Manchester, R. N., & Johnston, S. 2007, *MNRAS*, in press (astro-ph/0703241)  
 Weltevrede, P. 2007, Ph.D. Thesis, Univ. of Amsterdam  
 Weltevrede, P., Stappers, B. W., & Edwards, R. T. 2006, *A&A*, 445, 243  
 Weltevrede, P., Edwards, R. T., & Stappers, B. W. 2007, *A&A*, in press

## APPENDIX A: A PROBABLE CAROUSEL SOLUTION

Our various observations also show an occasional  $0.20 c/P_1$  modulation feature, and in a 200-pulse interval of PS A (in Table 1) both it and the low frequency feature appear prominently. As discussed above, the “local” value of the putative  $\hat{P}_3$  feature here is some  $28.44 P_1$ , whereas the  $P_3$  modulation period can be measured from the LRF to be  $5.22 \pm 0.01 P_1$ . However, the harmonic resolved fluctuation spectrum of Figure A1 shows that this feature probably represents a first-order alias of its true frequency, making its period  $1.237 \pm 0.011 P_1$ . A simple calculation will show that the aliased  $P_3$  value is incommensurate with  $28.44 P_1$ , but the first-order alias is precisely  $1/23$  of it.

These circumstances strongly suggest that B1133+16’s subbeam carousel very occasionally exhibits a semi-stable, characteristic pattern in which many of the beamlets have an azimuthal spacing of ( $360^\circ/23 =$ )  $15.6^\circ$ . Usually, though, this characteristic spacing is not sufficiently represented to produce a  $P_3$  feature.

Using a knowledge of the pulsar’s basic emission geometry (*e.g.*, Rankin 1993b), the central longitude, and the (first-order aliased!) drift direction, we can construct a subbeam carousel map using the cartographic transform method developed by Deshpande & Rankin (2001). The resulting map is shown and described in Figure A2. Note the many instances in which bright beamlets are spaced by the characteristic  $16^\circ$ , although one would be hard pressed to count any 23 beamlets in this map!

This carousel solution, of occasional pertinence at best, is interesting in several respects. First, even this most orderly interval in our several PSs is hardly so. About the most that can be said for it is that many beamlets appear to be spaced by roughly the  $360^\circ/23$  value. Perhaps, however, spacings near this amount are favored overall. If so, it is also interesting that beamlets sweeping through our sightline with this spacing are undersampled or aliased by the star’s rotation rate. Aliasing exaggerates the irregularities in any time sequence and can quickly produce a randomized appearance. Perhaps this circumstance is partly responsible for the difficulties of many observers over many years to find order in the PSs of this brightest of the Cambridge pulsars.

This paper has been typeset from a  $\text{\TeX}/\text{\LaTeX}$  file prepared by the author.

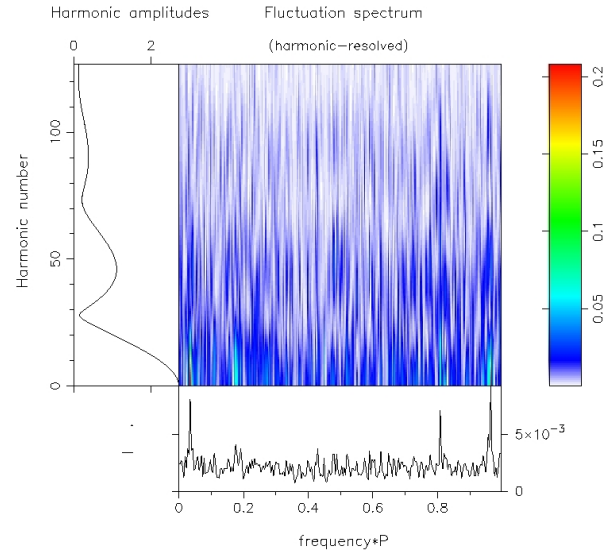


**Figure A1.** Harmonic resolved fluctuation spectrum (see Deshpande & Rankin 2001 for a full explanation) for the first 600 pulses of observation A (in Table 1). Here we see both the putative  $28.44 P_1$  circulation-time feature and the  $5 P_1$  “drift” feature. Note that the former is primarily amplitude modulated, whereas the latter is both first-order aliased and almost entirely phase modulated. See text.

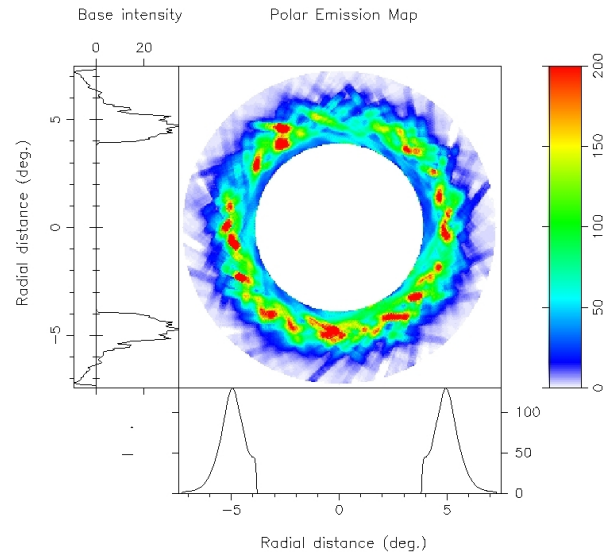


**Figure A2.** Polar map constructed using pulses 242-504 of the A PS. Here,  $\hat{P}_3$  was determined to be  $28.44 P_1$ , so the average of 7 carousel rotations is depicted. The magnetic axis is at the centre of the diagram, the “closer” rotational axis is upward, and (assuming a positive or equatorward traverse) the sightline track sweeps through the lower part of the pattern. Here, the star would rotate clockwise, causing the sightline to cut the counter-clockwise-rotating subbeam pattern from right to left; see DR01 for further details. The side panels give the “base” function (which has not been subtracted from the map), and the lower panel shows the radial form of the average beam pattern.